ACSNANO

www.acsnano.org

Article

# Noninvasive, Rapid, and Precise Identification of Esophageal Cancer via Salivary Extracellular Vesicle-Based Diagnosis

Liu Huang,[¶] Meng Li,[¶] Wenpeng Liu, Doudou Lou, Qingfu Zhu, Tony Y. Hu,* Luke P. Lee,* and Fei Liu*

Cite This: https://doi.org/10.1021/acsnano.5c20621

Read Online

ACCESS | Metrics & More | Article Recommendations | Supporting Information

**ABSTRACT:** Salivary extracellular vesicles (EVs) have been recognized as one of the most promising noninvasive sources of biomarkers for early cancer detection. However, the lack of efficient isolation and accurate identification methods for salivary EVs limits their clinical utility in early cancer diagnosis. Here, we report the rapid and precise identification of esophageal cancer using the Saliva Extracellular vesicle-based Early Diagnostic system (SEEDx). In this system, salivary EVs were isolated, purified, amplified, and analyzed from human saliva by integrating the ultrafast-isolation platform EXODUS with tandem mass tag (TMT)-based proteomics analysis (EXODUS-TMT proteomics). Using TCGA esophageal cancer (EC) and GTEx healthy population cohorts, we developed a diagnostic model consisting of 9 markers (HIST2H2BE, TP53BP2, TPM4, CALR, HDGF, LMNA, GUSB, NADSYN1, and AGRN), which demonstrated high diagnostic accuracy with AUC values of 0.996 for EC and 0.991 for early-stage EC. We further established a cost-effective model using only two markers (HDGF and CALR) to diagnose both EC and early-stage EC, achieving AUC values of 0.950 and 0.935, respectively. This model was validated in an independent, prospectively collected cohort of EC patients, yielding AUC values of 0.873 and 0.854, respectively. Our streamlined EV isolation and identification workflow facilitates noninvasive biomarker discovery for early-stage esophageal cancer detection. This study extends the EXODUS platform to salivary EVs for EC detection, documents matrix-specific workflow optimizations, and identifies saliva-derived biomarker signatures integrated into a multimarker diagnostic model.

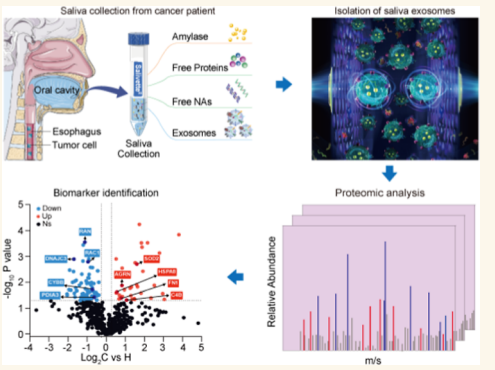


**KEYWORDS:** *salivary EVs, label-free isolation, biomarker discovery, esophageal cancer detection, early cancer diagnosis*



## 1. INTRODUCTION

Esophageal cancer (EC) is one of the most aggressive malignancies of the gastrointestinal tract and the sixth leading cause of cancer-related mortality worldwide.[1] More than half of global EC cases occur in China. Due to its insidious onset, nonspecific early symptoms, and the lack of rapid and sensitive diagnostic techniques, approximately 70% of patients are diagnosed at advanced stages.[2] In China, the 5-year survival rate for advanced EC is less than 10%, whereas it can increase to 86% when the disease is detected at an early stage.[3]

Gastroscopy-based tissue biopsy remains the gold standard for EC diagnosis. However, its widespread use in population screening is limited by accessibility, invasiveness, repeatability, cost, time requirements, and potential clinical complications. Therefore, tissue biopsy alone is insufficient for large-scale screening. The discovery and application of specific biomarkers through noninvasive diagnostic approaches would provide substantial scientific and clinical value for early EC detection.

Human saliva represents a promising source for noninvasive cancer diagnostics.[4] Saliva can be collected easily and allows repeated samoling, in contrast to other body fluids such as blood[5] and cerebrospinal fluid.[6,7] Salivary extracellular vesicles (EVs) carry diverse cancer-related multiomics biomarkers and have been assocated with both head and neck tumors (e.g., oral cancer)[8] and distant malignancies such as lung,[9] pancreatic,[10] and breast cancers.[11] Although tumor-specific biomarkers derived from salivary EVs have not yet reached toutine clinical application, they show considerable promise for early EC detection. For example, Lin et al. identified and validated chimeric mRNA derived from salivary EVs as a biomarker for both early and late EC detection.[12] Xie et al. reported significant upregulation of miR-10b, miR-144, and miR-451 in saliva samples from EC patients.[13] Beyond transcriptomic analysis, proteomic profiling of salivary EVs may further facilitate the identification of EC-related biomarkers for noninvasive diagnosis.

Received: November 25, 2025
Revised: February 13, 2026
Accepted: February 17, 2026

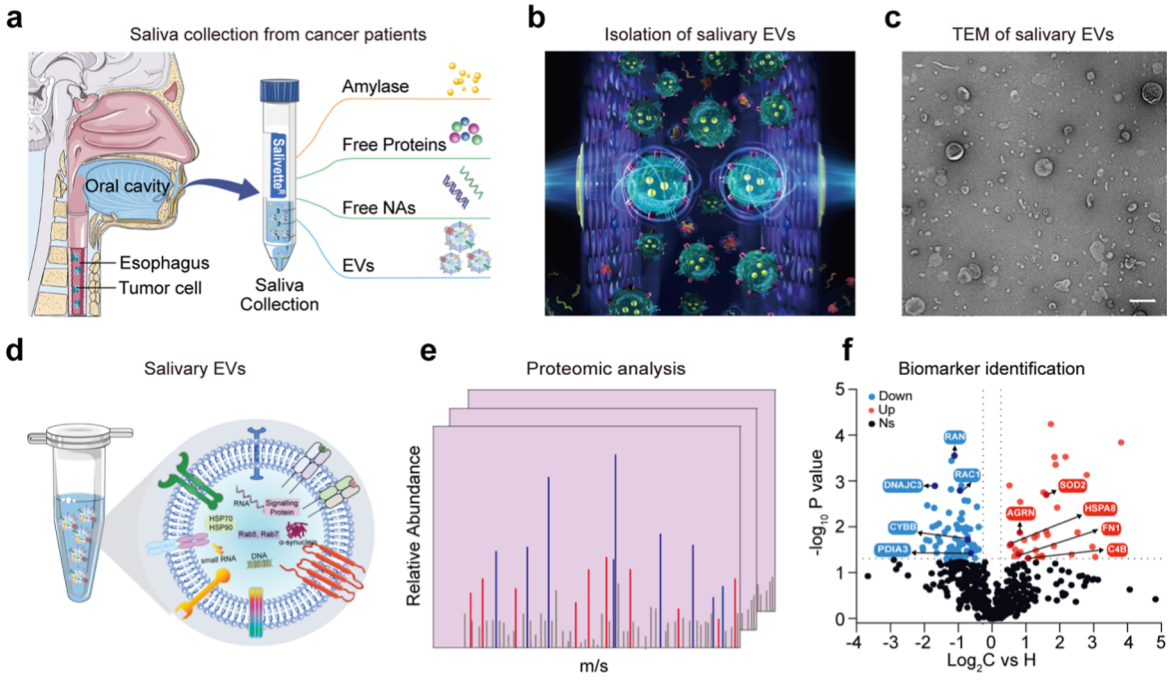


**Figure 1.** Schematic illustration of EXODUS-TMT proteomic method for analyzing salivary EVs. (a) Saliva was collected from healthy donors and patients with EC. (b) The salivary EVs were isolated using EXODUS based on negative pressure oscillation and nanoporous membrane, and the refrain double-coupled harmonic oscillator enabled membrane vibration. (c) The morphology of salivary EVs based on TEM. (d) Schematic diagram of collected salivary EVs. (e) Quantitative proteomic analysis of salivary EVs via TMT. (f) Identification of salivary EV protein biomarkers.

Tandem mass tag (TMT)-based quantitative proteomics is a powerful approach for cancer marker discovery, offering high sensitivity, accuracy, and reproducibility. However, efficient separation and purification of EVs from crude saliva remain major challenges for downstream proteomic analysis.[14] Despite growing interest in salivary EVs as diagnostic biomarkers, labor-intensive and inefficient isolation methods hinder their clinical translation.

Currently, the most commonly used methods for isolating salivary EVs include ultracentrifugation (UC)[15] and polymer-based precipitation.[16−18] However, UC is time-consuming (>3 h), requires large sample volumes, produces relatively low yields, and may alter EV morphology and biological function. Polymer precipitation methods, such as polyethylene glycol (PEG), can introduce protein and polymer contamination, making them unsuitable for downstream proteomic analysis.[7] More recently, acoustofluidic approaches have been developed for EVs separation from plasma, but their capacity to process complex and large-volume samples remains limited. We previously reported the ultrafast isolation system for exosome detection (EXODUS),[19] which enables rapid extraction of high-purity, high-yield, and structurally intact EVs from clinical samples.[20]

In this study, we presents SEEDx, a saliva-based extracellular vesicle diagnostic platform for esophageal cancer. By integrating EXODUS with tandem mass tage (TMT)-based quantitative proteomics, we achieved efficient isolation purification, amplification, and detection of EVs from human saliva. Using EXODUS, major salivary proteins such as albumin and amylase levels were substantially reduced, while EV yield was significanlly increased, providing sufficient material for downstream proteomic analyses. To evaluate EV purification efficiency, we compared EXODUS with conventional UC and PEG methods using Western blot (WB), nanoparticle tracking analysis (NTA), and transmission electron microscopy (TEM). The EXODUS-TMT platform was then applied to identify protein biomarkers for EC diagnosis from purified salivary EVs. Diagnostic models were subsequently validated using the TCGA EC cohort, the GTEx healthy population cohort, and an independent prospectively collected validation cohort from Tongji Hospital. Our findings demonstrate the feasibility of accurate clinical EV-based diagnostics through the integration of the EXODUS-TMT platform. Importantly, this work extends the application of EXODUS to saliva, a significantly more complex biological matrix than plasma, requiring specicalized pretreatment strategies to address viscosity and mucin content. Rather than introducing hardware innovations, our contribution lies in matrix-specific workflow optimization and the identification of saliva-derived EV biomarkers for EC detection.

In particular, this study establishes a matrix-tailored workflow for salivary EV isolation and identifies saliva-specific biomarker signals that are integrated into a multimarker diagnostic model. It represents the first demonstration of EXODUS-based isolation of salivary EVs for cancer diagnostics, enabling a noninvasive diagnostic stragety beyond traditional blood-based assays.[21] Future studies are warranted to evaluate the feasibility feasibility, cost-effectiveness, and implementation pathways of this approach in real-world screening settings. This analytical and clinical pipeline follows established biomarker development practices, involving high-throughput proteomic discovery followed by targeted validation in an independently cohort.


https://doi.org/10.1021/acsnano.5c20621
ACS Nano XXXX, XXX, XXX−XXX

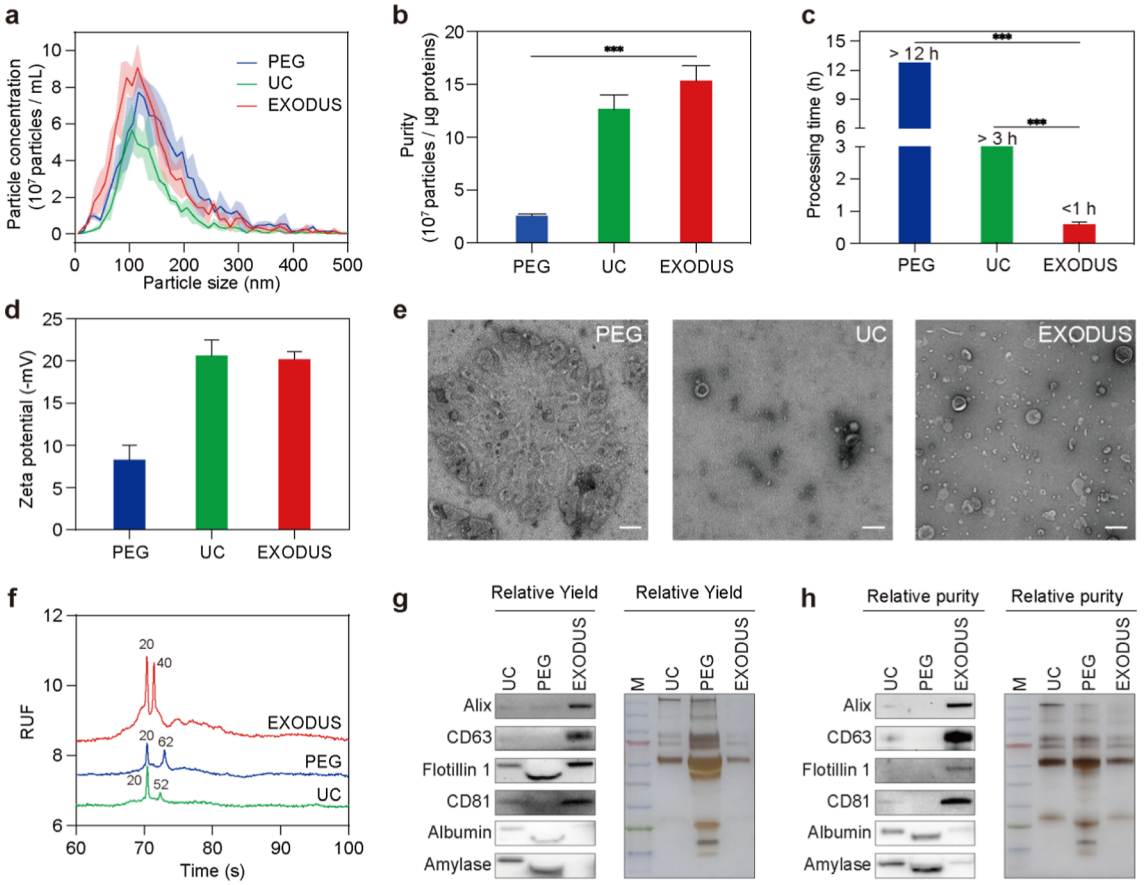


**Figure 2.** Characterization of EVs isolated from human saliva. (a) Size distribution and concentration of particles using NTA. (b) Comparison of salivary EVs purity. (c) Salivary EVs isolation time for PEG, UC, and EXODUS. (d) Zeta potential of salivary EVs. (e) TEM images of salivary EVs. Scale bar = 200 nm. (f) Electropherograms of EV RNA profiles based on different methods. (g) Equal-volume (35 $\mu$L) and (h) equal-mass (2 $\mu$g) gel-loading was used to evaluate the relative yield and relative purity of salivary EVs (for WB and staining, respectively). M = molecular weight marker. (*, $p < 0.05$;**, $p < 0.01$; ***, $p < 0.001$).

## 2. RESULTS AND DISCUSSIONS

### 2.1. Illustration of EXODUS-TMT Proteomics Analysis for Biomarker Identification from Salivary EVs

The principles and workflow of the EXODUS-TMT proteomic analysis platform are illustrated in Figure 1. After collecting saliva samples from 3 healthy donors and 3 EC patients (Figure 1a), EXODUS was applied to rapidly purify EVs from human saliva with high purity (Figures 1b and S1). Figure 1c demonstrates the rapid isolation of EVs with high yield, high purity, and high stability using EXODUS. The purified and enriched salivary EVs (Figure 1d) were subsequently subjected to TMT-based proteomic analysis for the discovery of protein biomarkers (Figure 1e,f).

### 2.2. Saliva-Specific Parameter Optimization for EXODUS EV Isolation

To accommodate the high viscosity and mucin content of saliva, we systematically optimized two core EXODUS parameters—negative pressure (−10 to −60 kPa) and conversion time (10−60 s)—using a standardized predilution protocol (1 mL saliva diluted to 5 mL) and two PBS washing steps. Processing time, NTA mean particle size and concentration, particle-to-protein ratio (purity), and Western blot readouts under both equal-mass and equal-volume loading conditions were evaluated to assess EV yield and purity. The mean particle size remained stable across all tested conditions. Increasing negative pressure shortened the processing time; however, particle number and purity declined when the pressure exceeded −30 kPa, likely due to increased transmembrane shear and membrane adsorption effects. Both EV purity and relative yield reached their maximum at −30 kPa. Conversion time had minimal influence on total runtime. EV purity and relative yield peaked at 10 s and subsequently exhibited a U-shaped trend with longer concersion times. Based on these results, −30 kPa negative pressure, a 10 s conversion time, and two PBS washes were selected as the default parameters for salivary EV isolation. Under these optimized conditions, both processing time and EV yield increased approximately linearly with the input volume (1−5 mL). Complete datasets and statistical analyses are provided in the Supporting Information (Figure S1a−k; methods in Supporting Information).

### 2.3. Comparison of Salivary EV Isolation Using EXODUS, UC, and PEG

We compared the efficiency of salivary EV isolation using EXODUS, UC, and PEG. NTA results showed that EXODUS yielded a higher concentration of salivary EVs, whereas PEG produced larger apparent particle sizes, likely due to the co-isolation of nonvesicular proteins (Figures 2a, S2a, Table S1, $p < 0.05$; Figure S6). Particle numbers and protein concentrations are shown in Figure S2b. EXODUS achieved a particle-to-protein ratio of ratio of $1.54 \times 10^8$ particles/$\mu$g


https://doi.org/10.1021/acsnano.5c20621
ACS Nano XXXX, XXX, XXX−XXX

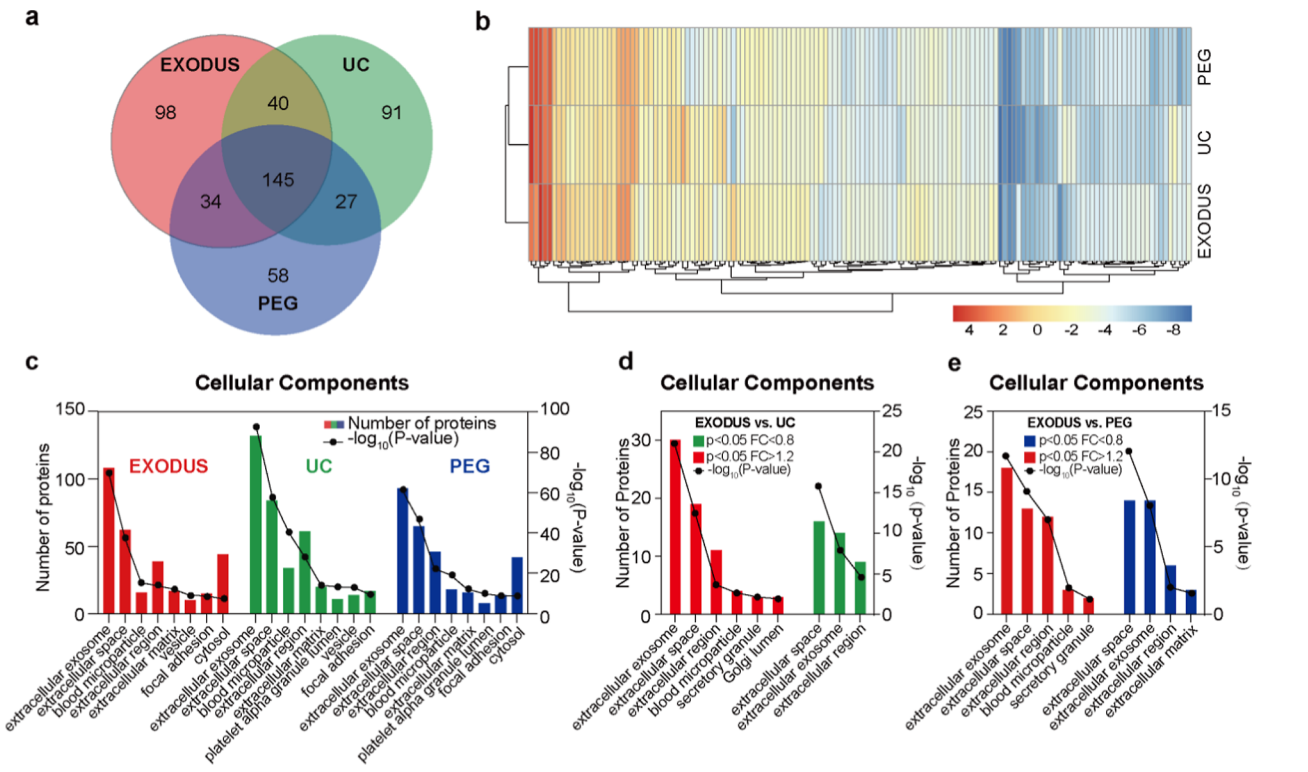


**Figure 3.** Qualitative analysis of salivary EV proteins. (a) The Venn diagram shows the number of proteins isolated using the EXODUS, UC, and PEG methods. (b) Clustered heatmaps show differences in the enrichment of shared proteins in salivary EVs isolated by different methods. Identified proteins in salivary EVs from the three isolation methods were analyzed by GO to determine their (c) cellular components. (Red represents EXODUS, green represents UC, and blue represents the PEG method). (d,e) GO annotation analysis of the differentially enriched proteins related to the cell components. (d) describes the EXODUS vs UC group, and (e) represents the EXODUS vs PEG group. (RED, GREEN, and BLUE represent the TMT-identified proteins of salivary EVs isolated by EXODUS, UC, and PEG, respectively).

protein, which was 5.95-fold higher than PEG and 1.21-fold higher than UC (Table S1). In addition, the processing time required to isolate salivary EVs from 1 mL saliva was only 35 min using EXODUS, compared with 3 and 12.5 h for UC and PEG, respectively (Figure 2c, Table S1). To further validate the reliability of EV quantification, consistent trends in particle concentration and yield were observed across three independent nanoparticle analysis platforms (Zetaview, NanoFCM, and Exoplorer), supporting the robustness of the EXODUS method in terms of both yield and purity (Figure S3).

We assessed salivary EV stability using zeta potential measurements and TEM analyses. EXODUS and UC-isolated salivary EVs exhibited a zeta potential of approximately −20 mV. PEG-isolated salivary EVs had a lower value of −7 mV (Figure 2d). This suggests that PEG-isolated salivary EVs had reduced particle dispersibility and tended to aggregate. TEM images confirmed significant aggregation in PEG-isolated salivary EVs due to coprecipitation with impurities. In contrast, UC and EXODUS-isolated salivary EVs displayed a homogeneous cup-shaped morphology with diameters ranging from 30-150 nm (Figure 2e). These TEM findings supported the results obtained from the zeta potential measurements.

We next evaluated the yield and length distribution of exosomal RNA after isolating salivary EVs using EXODUS, UC, and PEG. The results showed that EXODUS enriched total exosomal RNA at levels approximately 5−10 times higher than those obtained using PEG and UC, respectively (Figure 2f). Gel electrophoresis was used to compare the relative yield and purity of salivary EVs under equal volume (35 $\mu$L) (Figure 2g) and equal mass (2 $\mu$g) (Figure 2h) loading conditions. Western blot (WB) analysis revealed higher expression levels of EV-assocated protein markers (Alix, CD63, Flotillin 1, CD81) in EVs isolated usingEXODUS. In contrast, the levels of non-EV salivary proteins (albumin, amylase) were significantly lower than those obtained by UC and PEG ($p < 0.05$) (Figures 2g, h and S2c, d, f, g). WB and staining analyses indicated a substantial reduction—rather than complete removal—of albumin and amylase inEXODUS-isolated EVs compared with UC and PEG. Compared with other purification strategies such as SEC, PS, andDGC, residual protein bands may still be visible under certain conditions. In contrast, higher levles of these containants were observed in UC- and PEG-based isolation samples (Figure 2g,h). These observations were further supported by silver staining results (Figure 2g, h).

Overall, EXODUS provided faster processing and higher EV yields while maintaining sufficient purity and stability for downstream analyses, offering clear efficiency and throughput advantages over UC and PEG.

In addition, we benchmarked EXODUS against other widely used EV isolation methods—including SEC, PS affinity, and DGC—using Western blot, particle-to-protein raio measurements, and processing-time metrics (Figures S4 and S5). These results indicate that EXODUS achieves higher yield with practical purity and shorter processing times, whereas SEC, PS, and DGC typically provide higher purity at the expense of longer processing and lower yields, reflecting a method-dependent purity−yield trade-off.


https://doi.org/10.1021/acsnano.5c20621
ACS Nano XXXX, XXX, XXX−XXX

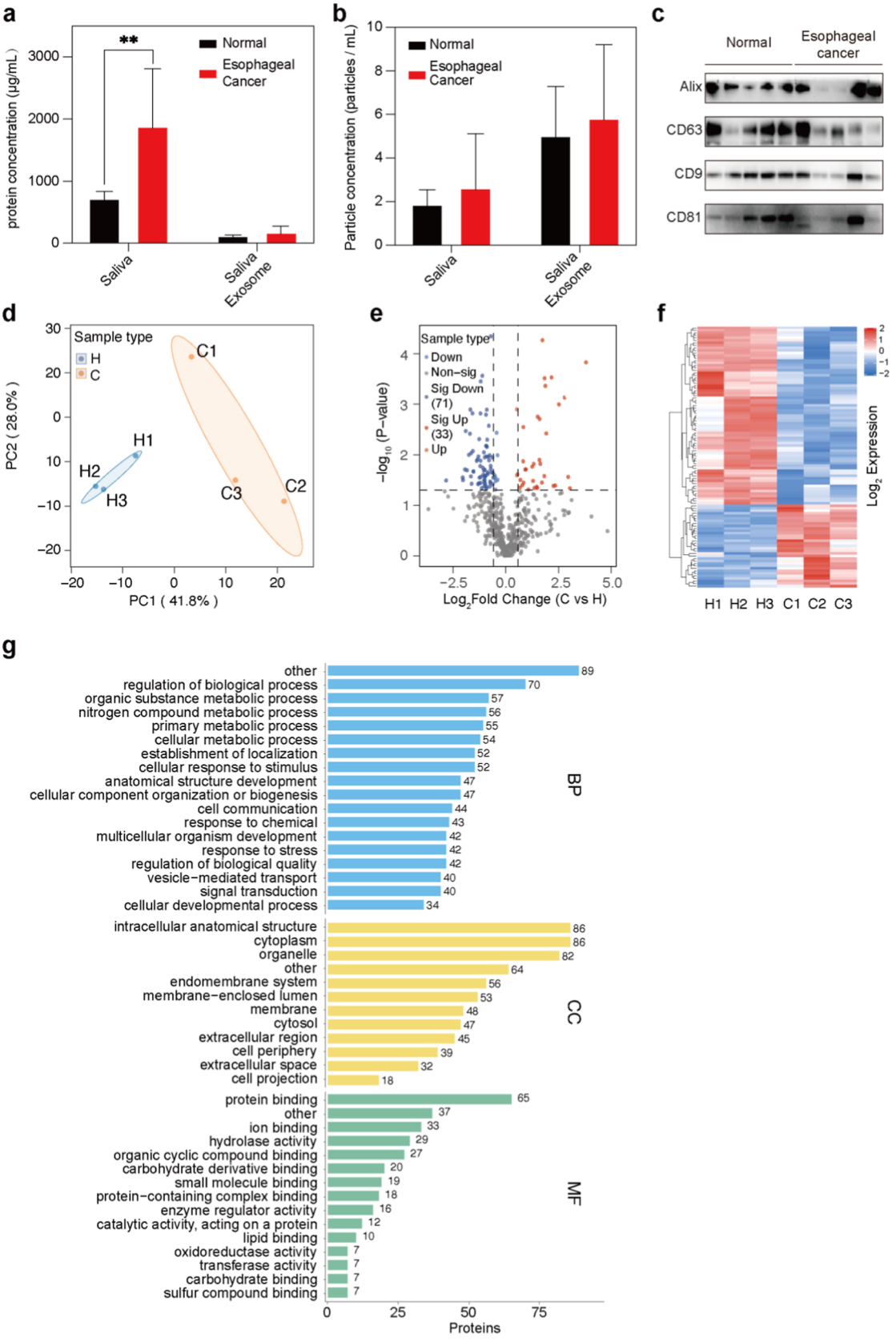


**Figure 4.** Isolation of salivary EVs from healthy donors and EC patients using EXODUS for proteomic analysis. (a) Raw salivary and EV protein concentrations of healthy controls and EC groups. (b) Initial saliva particle concentration and salivary EV concentration in the healthy control and EC groups. (c) WB was used to evaluate the protein expression of salivary EVs in the healthy control and EC groups. (d) Two-dimensional scatter plot of principal component analysis. (e) Quantitative volcano chart. (f) Cluster heatmap of differentially expressed proteins in the EC and healthy control groups ($p < 0.05$). The heatmap color key displays the row z-score. (g) The statistical distribution of different proteins in the GO secondary classification.


https://doi.org/10.1021/acsnano.5c20621
ACS Nano XXXX, XXX, XXX−XXX

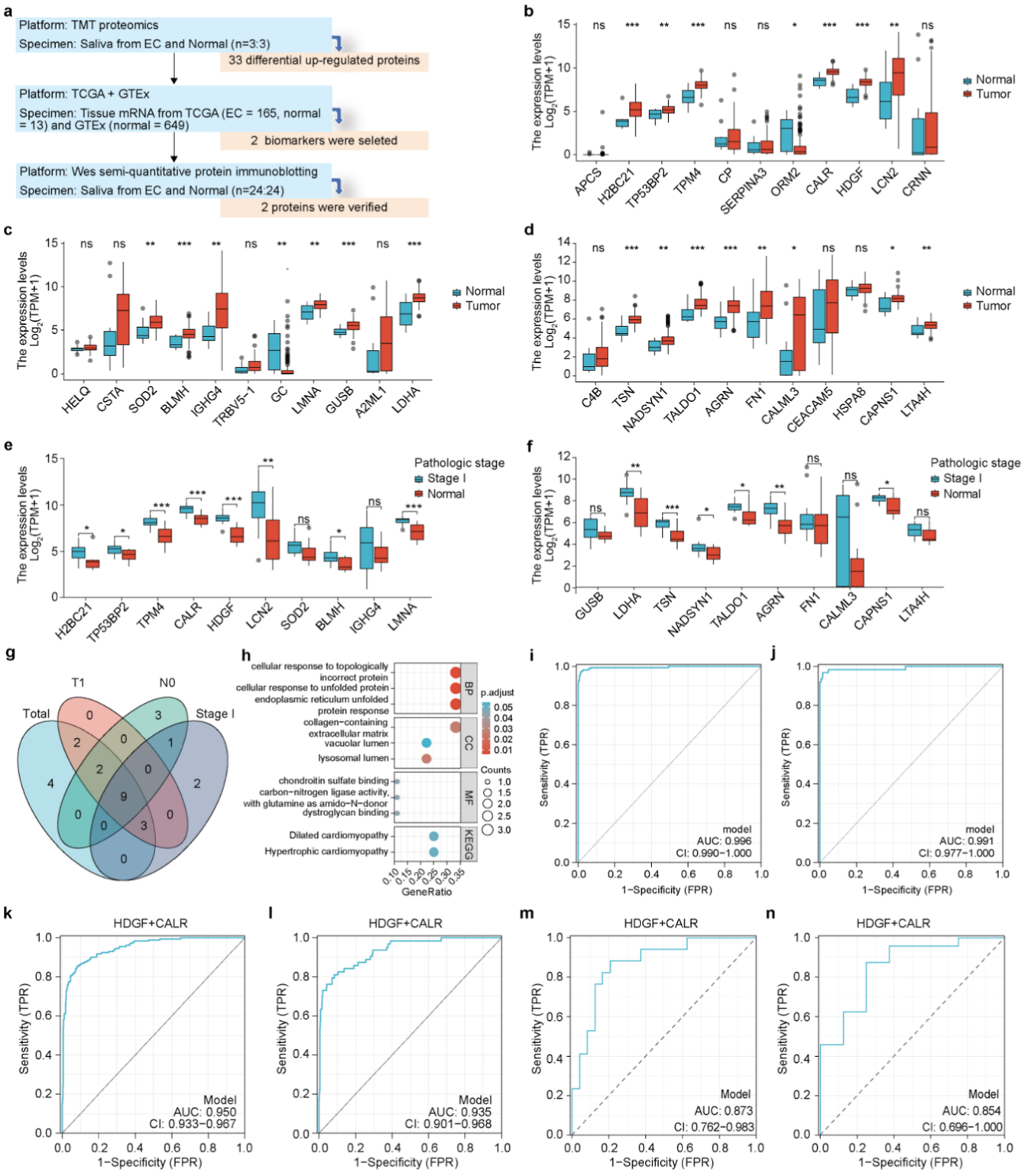


**Figure 5.** Bioinformatic analysis of differentially upregulated proteins in EC patients along with screening and validation of diagnostic markers. (a). The flowchart of the study. (b–d) Differential expression analysis of the 33 upregulated salivary EV proteins in TCGA EC tissues and normal tissues (ns, $p \geq 0.05$; *, $p < 0.05$; **, $p < 0.01$; ***, $p < 0.001$). (e–f) Differential expression analysis in stage I EC tissues and normal tissues (ns, $p \geq 0.05$; *, $p < 0.05$; **, $p < 0.01$; ***, $p < 0.001$). (g) The Venn diagram description showed that the mRNA of 9 exosomal proteins (HIST2H2BE, TP53BP2, TPM4, CALR, HDGF, LMNA, GUSB, NADSYN1, AGRN) was upregulated in both EC and early stage EC tissues when compared to 11 normal tissues coming from EC patients. (h) KEGG annotation analysis of HIST2H2BE, TP53BP2, TPM4, CALR, HDGF, LMNA, GUSB, NADSYN1, and AGRN. The size of the bubble corresponds to the gene counts enriched in the pathway. The bubble color indicated the *p*-value after multiple comparisons. Receiver Operating characteristic (ROC) analysis was conducted to evaluate the diagnostic value of the 9-gene model for all EC (i) and stage I/IIA EC (j) patients as well as the 2-gene model (HDGF plus CALR) for all EC (k) and stage I/IIA EC (l) patients by comparing the TCGA-EC cohort ($n = 165$) to GTEX- healthy control cohort ($n = 649$). Furthermore, ROC analysis was performed for the 2-gene model in EC (m) and stage I/IIA EC patients (n) of the validation cohort.


https://doi.org/10.1021/acsnano.5c20621
ACS Nano XXXX, XXX, XXX−XXX

### 2.4. Qualitative and Quantitative Proteomics of Salivary EV Proteins

Label-free quantitative proteomics was performed to analyze salivary EV proteins isolated using EXODUS, UC, and PEG. A total of 493 proteins were identified and quantified across the three isolation methods, of which 49.9% (246 proteins) were shared among all datasets (Figure 3a, Table S2). Among these, 145 proteinswere commonly detected in salivary EVs isolated by all three methods and were further analyzed using hierarchical clustering and heatmaps visualization. Although the same proteins were detected in EVs isolated by different methods, notable differences were observed in their relative enrichment levels (Figure 3b). These results suggest that different isolation techniques influence the enrichment profiles of salivary EVs proteins, potentially affecting downstream proteomic analyses and biomarker discovery.

Gene Ontology (GO) analysis indicated that "extracellular exosome" was the predominant cellular component across all three isolation methods (Figure 3c), confirming that each method effectively enriched salivary EVs. However, the number of EV-related proteins identified in the EXODUS dataset appeared lower than that in the UC group. This discrepancy was primarily due to a higher number of protein accessions that were not recognized by the DAVID database during annotation. Specificanlly, 143 proteins in the EXODUS dataset lacked annotation (i.e., were not mapped to *Homo sapiens entries*), compared with 125 proteins in the UC dataset (Table S3).

Biological Process (BP) analysis revealed that the most abundant proteins across all three groups were associated with immune response, suggesting that immune regulation represents a dominat biological process in salivary EVs. Additional enriched processes included defense salivary EVs were involved in defense responses to bacteria and fungi, nucleosome assembly, and bitter taste perception (Figure S7a). Molecular Function (MF) analysis indicated that the most enriched functional categories included structural constituents of chromatin, protein heterodimerization activity, antigen binding, and lipid binding (Figure S7b). Qualitative comparison showed greater consistency between EXODUS and UC in the salivary EV proteins profiles than with PEG. GO cellular component enrichment further demonstrated that proteins isolated using EXODUS were primarily localized to extracellular vesicles, extracellular space, and extracellular regions. Notably, EXODUS exhibited higher enrichment of EV-related protein classes compared with UC and PEG, suggesting an advantage for disease-related biomarker discovery (Figure 3d,e).

MF analysis of EXODUS-isolated salivary EVs further showed stronger enrichment of proteins associated with chromatin structural constituents, protein heterodimerization, binding activities related to DNA, antigen, lipids, and lipopolysaccharides compared with UC and PEG (Figure S7c,e), indicating better preservation of protein functionality during isolation. Similarly, biological process (BP) enrichment analysis revealed that proteins in EXODUS-isolated EVs were significantly associated with immune response, antibacterial humoral response, defense response to bacteria, and nucleosome assembly (Figure S7d,f), highlighting their potential involvement in antibacterial and defense mechanisms within the oral environment. Overall, salivary EV proteins isolated using EXODUS contained a higher proportion of functionally relevant proteins associated with key cellular processes, demonstrating the effectiveness of the EXODUS-TMT proteomics platform for comprehensive EV protein analysis.

### 2.5. Investigation of Isolated Salivary EVs from Patients with Esophageal Cancer (EC)

To compare the characteristis of salivary EVs between healthy donors and EC patients, including particle size, protein concentration, and marker expression, we collected 1 mL saliva samples from 5 individuals in each group and isolated salivary EVs using EXODUS (Table S4). The total salivary protein concentration was significantly higher in EC patients than in healthy controls (Figure 4a; $p < 0.05$). NTA further showed higher particle concentrations in both whole saliva and isolated salivary EVs from the EC group compared with the healthy group (Figure 4b). The average particle size did not differ significantly between the two groups (Figure S8a). However, slightly longer processing times were required to isolate salivary EVs from EC patients, likely due to increased saliva viscosity. WB analysis (Figures 4c and S8b) demonstrated comparable enrichment of canonical EV markers (Alix, CD63, CD9, CD81) in both groups (all $p < 0.05$). Notably, substantial varability in protein and particle concentrations was observed among EC patients, reflecting interpatient heterogeneity.

EXODUS was used to isolate EVs from saliva samples obtained from 3 EC patients and 3 healthy donors (2 mL per sample) to further investigate proteomic differences between salivary EVs from EC patients and healthy individuals (Table S5). TMT proteomic analysis identified a total of 657 proteins, among which 519 proteins were quantified (Table S6). To evaluate the reproducibility of the quantitative proteomic data, principal component analysis (PCA) and Pearson correlation coefficient (PCC) analyses were performed on the normalized dataset. As shown in Figure 4d, PCA revealed clear separation between the EC and healthy groups (PC1 = 41.8%, PC2 = 28.0%) and tight clustering within each group, with 95% confidence ellipses indicating low intragroup varability. Consistently, the PCC heatmap (Figure S8c) demonstrated strong correlations among biological replicates within the same group (e.g., H2 vs H3: $R = 0.95$, $p < 0.001$; C2 vs C3: $R = 0.56$, $p < 0.05$). These results confirm the reproducibility and reliability of the quantitative proteomic measurements. Differential expression analysis identified 33 proteins that were significantly upregulated in EC-derived EVs (fold change $\geq 1.5$ and $p < 0.05$) and 71 proteins that were significantly downregulated (fold change $\leq 1/1.5$ and $p < 0.05$) (Figure 4e and Table S7). Hierarchial clustering based on the expression profiles of these differentially expressed proteins clearly distinguished the EC group ($n = 3$) from healthy controls ($n = 3$) (Figure 4f). To further expore the biological relevance of these differential proteins, GO secondary annotations analysis was performed (Figure 4g and Tables S8, S9). BP enrichment analysis (green) revealed that several upregulated proteins—including FN1, HSPA8, CALR, AGRN, IGHG4, LMNA, SOD2, SERPINA3, C4B, and CAPNS1—were primarily associated with immune response and related biological processes (Tables S8 and S9).

### 2.6. Validation of Upregulated Proteins in TCGA EC Cohorts

The workflow for EC biomarker discovery and validation is illustrated in Figure 5a. The 33 upregulated proteins identified from the proteomic analysis were further evaluated in TCGA


https://doi.org/10.1021/acsnano.5c20621
ACS Nano XXXX, XXX, XXX−XXX

EC cohorts, including normal tissues ($n$ = 13) and tumor tissues ($n$ = 165). Among these candidates, the mRNA expression levels of 20 proteins were significantly higher in tumor tissues than in normal tissues (Figure 5b−d, ns, $p \geq 0.05$; *, $p < 0.05$; **, $p < 0.01$; ***, $p < 0.001$). Stage-specific analysis further showed that 16 markers were significantly upregulated in stage T1 EC tissues ($n$ = 27) compared with normal tissues (Figure S9a,b). Similarly, 15 markers were elevated in stage N0 EC tissues ($n$ = 66) (Figure S9c,d), and 15 markers were significantly upregulated in TNM stage I EC tissues ($n$ = 17) relative to normal tissues (Figure 5e−f). Notably, 9 markers showed consistently higher expression in both EC tumors and early-stage EC compared with normal tissues. These markers included H2BC21, TP53BP2 (Tumor Protein P53 Binding Protein 2), TPM4 (Tropomyosin 4), CALR, HDGF, LMNA, GUSB, NADSYN1, and AGRN (Figure 5g). Clinical and demographic information for the prospective EC cohort used in the validation study is provided in Supplementary Table S10.

### 2.7. KEGG Pathway Enrichment Analysis of the 9 Makers for Early Stage EC

KEGG pathway enrichment analysis was performed to elucidate the functional roles of the identified proteins. The results showed that the 9 differentially upregulated proteins (HIST2H2BE, TP53BP2, TPM4, CALR, HDGF, LMNA, GUSB, NADSYN1, and AGRN) were significantly enriched in pathways related to the endoplasmic reticulum unfolded protein response, cellular response to unfolded or misfolded proteins, collagen-containing extracellular matrix, lysosomal lumen, and vacuolar lumen. Functional annotations further indicated that these proteins were associated with dystroglycan binding, carbon−nitrogen ligase activity acting on amido groups and chondroitin sulfate binding. In addtion, KEGG pathway analysis linked these proteins to cardiomyopathy-related pathways, including hypertrophic and dilated cardiomyopathy (Figure 5h).

### 2.8. Receiver Operating Characteristic (ROC) Analysis for Diagnosing EC and Early-Stage EC

To further evaluate the diagnostic performance of the 9 candidate biomarkers (HIST2H2BE, TP53BP2, TPM4, CALR, HDGF, LMNA, GUSB, NADSYN1, and AGRN) , mRNA expression profiles from 649 healthy individuals in the Genotype-Tissue Expression (GTEx) dataset were used as controls. Because of the limited number of cases in certain EC stages, stages I and IIA were combined and defined as early-stage EC ($n$ = 62). Receiver operating characteristic (ROC) and area under the curve (AUC) analyses demonstrated that the 9-marker signature achieved excellent diagnostic performance for both EC and early-stage EC, with AUC values of 0.996 and 0.991, respectively (Figure 5i,j). For EC diagnosis,the logistic regression (LR) model was (−4.2176 + −0.6406 ×HIST2H2BE + 2.6864 × TP53BP2 + −2.825 × TPM4 + 3.3437 × CALR + −0.2341 × HDGF + −0.4377 × LMNA + −1.6571 × GUSB + −4.069 × NADSYN1 + 5.2665 × AGRN) with a cutoff value of −1.064, the model achieved a sensitivity of 0.976 and a specificity of 0.983 (Figure 5i). For early-stage EC ( stage I/IIA), the LR model was (−4.8237 + −0.9149 × HIST2H2BE + 2.7415 × TP53BP2 + −2.841 × TPM4 + 3.8294 ×CALR + −1.1903 × HDGF +0.3948 ×LMNA + −2.1644 ×GUSB + −3.6601 × NADSYN1 + 4.7928 × AGRN) with a cutoff value of −1.769, this model achieved a sensitivity of 0.968 and a specificity of 0.985 (Figure 5j). Several of these markers have known biologial relevance to cancer. TP53BP2 regulates apoptosis and cell growth through interactions TP53.[22] TPM4 has been reported to have the strong diagnostic value in ESCC.[23] CALR is an endoplasmic reticulum-resident -binding protein involvedthat binds to $Ca^{2+}$ involved in malignant transformation, tumor progression, and response to cancer therapy.[24] HDGF promotes cancer cell transformation, angiogenesis, and metastasis and can be detected at elevated levels in the serum of cancer patients.[25] LMNA encodes lamin proteins that regulate nuclear stability, chromatin organization, and gene expression.[26] GUSB, NADSYN1, and AGRN encode $\beta$-glucuronidase, NAD Synthetase 1, and Agrin, respectively.

To develoop a more cost-effective diagnostic model, we further reduced the number the number of markers while maintaining acceptable diagnostic accuracy. Based on AUC ranking (Table S11), the 2 top-performing markers, HDGF and CALR, were selected for further analysis. The two-marker model also showed strong diagnostic performance, with AUC values of 0.950 for EC and 0.935 for early-stage EC (Figure 5k, l). For EC diagnosis, the LR model was (−39.0605 + 2.9781 × CALR +1.7188HDGF). With a cutoff value of −0.885, the model achieved a sensitivity of 0.852 and a specificity of 0.920. For early-stage EC diagnosis, the LR model was (−38.2253 + 2.8100 × CALR +1.6754 × HDGF). With a cutoff value of −1.867, the model achieved a sensitivity of 0.810, and a specificity of 0.917. These results demonstrate the strong diagnostic potential of salivary EV-derived biomarkers for both EC and ealy-stage EC detection.

### 2.9. Validation of Diagnostic Accuracy for EC and Early-Stage EC in an Independent Prospectively Cohort

Saliva samples were prospectively collected from 24 healthy volunteers and 24 newly diagnosed EC patients to validate the prespecified diagnostic models; no longitudinal follow-up was performed (Table S10). EC patients exhibited higher particle concentrations and total protein levels in saliva than healthy controls (Figure S8,f). Because HDGF and CALR expression data were unavailable for 7 EC patients, the final analysis included 17 EC patients (8 with stage I/IIA disease and 9 with stage IIB-IIIB disease), as shown in Figure S8g,h. The relative protein aboundances of both HDGF and CALR were higher in EC patients than in healthy individuals (Figure S8i,J). For EC diagnosis, the combined HDGF + CALR biomarker panel achieved an AUC of 0.873 (95% CI: 0.762−0.983), with asensitivity of 0.882 and a specificity of 0.792 (Figure 5m). For early-stage EC (stage I/IIA), the biomarker panel yielded an AUC of 0.854 (95% CI: 0.696−1.000), with a sensitivity of 0.875 and a specificity of 0.750 (Figure 5n). To date, few salivary biomarkers have demonstrated comparable sensitivity and specificity for early-stage EC detection. Previous studies have reported the diagnostic potential of blood-derived exosomal biomarkers for esophageal cancer. For example, plasma exosomal proteins (CD14, AUC = 0.96),[27] metabolites[28] (3′-UMP/palmitoleic acid/palmitaldehyde/isobutyl decanoate; AUC = 0.98), and miRNAs[29,30] (miR-25−3p, AUC = 0.932; miR-23b-3p, AUC = 0.708;[29] miR-636/miR-7641/miR-1246/miR-28−3p[30] panel, AUC = 0.802) have shown diagnostic value. Serum or plasma exosomal lncRNAs[31,32] (CHI3L1/MMP13/SPP1, AUC = 0.918; POU3F3/SCCA,[32] AUC = 0.926) and circulating miRNA panels[33] (miR-103/miR-106b/miR-151/miR-17/miR-181a/miR-21/miR-25/miR-93, AUC = 0.83) have also been


https://doi.org/10.1021/acsnano.5c20621
ACS Nano XXXX, XXX, XXX−XXX

reported. Across these studies, sensitivities ranged from 66.13 to 90.50% and specificities from 71.31 to 94.20% (Table S12).[27−34] Compared with blood-based assays, salivary EV biomarkers offer several advantages, including noninvasive sampling, improved patient comfort, and simpler collection procedures. These features enable repeated sampling and may facilitate home-based sample collection; however, the feasibility of large-scale community screening requires further investigation. Notably, this validation did not include benign esophageal diseases or multicenter cohorts. In addition, real-world screening protocols, cost-effectiveness, and implementation feasibility were not evaluated. Therefore, the borader clinical utility of this approach beyond hospital-based diagnostic settings remains to be established.

Unlike our previous plasma-based study, which focused on a single blood EV marker,[21] the present work implements a matrix-optimized workflow for saliva EV analysis. This workflow integrates EXODUS-based EV isolation with TMT-based quantitative proteomics followed by multimarker model development. The analytic pipeline follows established biomarker discovery practice and is applied here to early EC detection in an independent, prospectively collected validation cohort.

## 3. CONCLUSION

Research on salivary EV-based biomarkers for the early diagnosis of esophageal cancer remains limited. In this study, we estabilished and validated an integrated platform combing EXODUS with tandem mass tag (TMT)-based quantitative proteomics (EXODUS-TMT Proteomics) for efficient for purification and comprehensive proteomic analysis of salivary EVs Compared with conventional UC and PEG precipitation methods, EXODUS enables noninvasive, automated, label-free, and rapid isolation of salivary EVs with high purity, yield, and reproduciblility, providing advantages in efficiency, sample quality, label-free, and cost. Proteomics analysis further demonstrated that salivary EVs isolated using EXODUS contain a higher proportion of EV-related protein markers. Through integrative proteomic screenning and transcriptomic validation, we identified 9 upregulated proteins (TP53BP2, TPM4, CALR, HDGF, HIST2H2BE, LMNA, GUSB, NADSYN1, and AGRN) that showed elevated expression in EC patients and were significantly associated early in TNM stage I or T1N0 EC patients from the TCGA cohort. Based on these markers, we constructed a 9-marker diagnostic model that achieved excellent diagnostic accuracy (AUC = 0.996 for EC and AUC = 0.991 for early-stage disease in the TCGA cohort. Based on these biomarkers, we constructed a 9 marker diagnostic model that achieved excellent diagnostic performance (AUC = 0.996 for EC and AUC = 0.991 for early-stage EC) in the TCGA EC cohort and the GTEx healthy population cohort.

To improve clinical practicality and reduce diagnostic costs, we further developed a simplified 2-marker model based on HDGF and CALR expression. This model demonstrated strong diagnostic performance, with AUC values of 0.950 for EC and 0.935 for early-stage EC. The robustness and validity of this model were further confirmed in an independent, prospectively collected validation cohort obtained from Tongji Hospital, achieving AUC values of 0.873 for EC and 0.854 for early-stage EC. Overall, the EXODUS-based EV isolation strategy combined with multimarker proteomic analysis provides a promising noninvasive approach for the early detection of EC.

This study has several limitations. First, although the SEEDx system demonstrated strong discrimination between EC patients and healthy controls, benign esophageal diseases were not included, which limits direct assessment of specificity against nonmalignant conditions. Future multicenter studies incorporating clinically well-characterized benign esophageal diseases will be essential for translational validation, consistent with established biomarker development frameworks. Second, the initial proteomic screening was conducted using a relatively small sample size, which limited the ability to formally evaluate potential confounding factors, such as age, at this exploratory stage. Nevertheless, stringent selection thresholds were applied, and candidate markers were subsequently evaluated using stage-stratified TCGA transcriptomic datasets as well as an independent prospectively collected validation cohort with a more balanced demographic distribution. These steps helped mitigate the risk of false discovery and demographic confounding. Finally, the present study primarily focused on diagnostic performance. Further studies are required to elucidate the biological mechanisms underlying the identifed biomarkers and to evaluate the feasibility and cost-effectiveness of implementing approach in real-world screening settings.

## 4. METHODS

### 4.1. Collection of Human Saliva

Both the test cohort and the independent, prospectively collected validation cohort were obtained from Tongji Hospital. Saliva samples were collected from healthy donors and patients between 9:00 am and 11:00 am from June 2022 to June 2023. The full study protocol was approved by the Ethics Committee of Tongji Hospital, Huazhong University of Science and Technology (Approval No. TJ-IRB20210329), and written informed consent was obtained from all participants. Inclusion Criteria for Healthy Subjects: (1) underwent regular annual physical examinations for at least 3 consecutive years without a history of malignant tumors. (2) Normal tumor marker levels. (3) Absence of malignant tumors confirmed by clinical examinations, including chest CT, breast ultrasound, abdominal and pelvic ultrasound, CT/ MRI, fecal occult blood testing, cervical smear in females, and gastrointestinal endoscopy within the past 3 years. (4) No history of general anesthesia or surgery within 1 month before sample collection. Inclusion Criteria for Esophageal Cancer Patients: (1) histologically confirmed primary esophageal squamous cell carcinoma. (2) No prior radical surgery or antitumor therapy (including radiotherapy, chemotherapy, targeted therapy, or immunotherapy) before sample collection. (3) No history of other malignant tumors or major systemic diseases. (4) No general anesthesia or surgery within 1month before sample collection. Participants were instructed to refrain from eating, drinking, or using oral hygiene products for at least 1 h before saliva collection. Each participant provided at least 6 mL of saliva, of which 1−2 mL was used for EV characterization and 4−5 mL for EV proteomics. Unstimulated saliva was collected using Salivette cotton swabs according to the manufacturer's protocol. Participants wree were instructed to remove the swab from the Salivette tube, place it in the mouth, and chew gently for approximately 60 s to stimulate salivation. The swab containing absorbed saliva was then returned to the Salivette tube. The samples were then centrifuged at 2,000 × *g* for 10 min (Rotor S-4−72, Centrifuge 5804 R, Eppendorf AG, Hamburg, Germany) to obtain a clarified saliva. During centrifugation, particles, cellular debris, and mucus strands were retained in the specially designed extended tip of the Salivette tube. The recovered supernatant saliva was used immediately for downstream analysis or stored at −80 °C until further processing. Samples used for model validation were prospectively collected from newly diagnosed EC


https://doi.org/10.1021/acsnano.5c20621
ACS Nano XXXX, XXX, XXX−XXX

patients and healthy controls. No longitudinal follow-up or outcome prediction was performed. Benign esophageal conditions (e.g., reflux esophagitis, Barrett's esophagus, benign strictures) were not enrolled; only histologically confirmed primary ESCC patients and healthy controls were enrolled.

### 4.2. Isolation of EVs from Saliva Using EXODUS

In brief, saliva samples were processed using the EXODUS workstation for automated EV isolation as follows: (1) Preprocessing of saliva samples. Freshly collected saliva was centrifuged at 12,000 × *g* (Rotor FA-45-24-11, Centrifuge 5424 R, Eppendorf AG, Hamburg, Germany) for 30 min at 4 °C to remove cells and debris. The supernatant was subsequently filtered using a 0.22 μm pore-size membrane filter (FPE-204-013, JET BIOFIL) to eliminate larger extracelluar vesicles, apoptotic bodies, and residual particles. (2) Device preparation. The EXODUS device was installed in the designated position on the EXODUS workstation and pre-rinsed twice with PBS (1 mL each time) prior to sample processing. (3) Parameter setup. All operating parameters were set to default values, including negative separation pressure, conversion time, single injection volume, injection frequency, and PBS washing frequency. (4) Sample loading. A 1 mL saliva sample was diluted to a final volume of 5 mL using 1× PBS. The diluted sample was transferred into a 50 mL centrifuge tube and placed in the designated position on the EXODUS workstation. The sample was then automatically introduced into the EXODUS device via an injection needle. (5) EV separation and collection. During operation, alternating negative pressure was applied across the two membranes within the EXODUS device to remove impurities, including free nucleic acids and proteins, while retaining salivary EVs within the chember. The purified EV fraction was subsequantly collected and concentrated to a final volume of approximately 200 μL.

### 4.3. Bicinchoninic Acid Assay

The total protein concentration of the isolated exosomes was determined using a bicinchoninic acid (BCA) protein assay kit (P0010S, Beyotime Biotechnology). Briefly, 0.8 mL of protein standard preparation solution was added to a tube containing protein standard (20 mg BSA) and mixted thoroughly until completely dissolved to abtain a 25 mg/mL stocksolution. An appropriate volume of this stock solution was then diluted to a final concentration of 0.5 mg/mL for standard curve preparation. For preparation of the BCA working solution, reagent A and reagent B were mixed at a ratio of 50:1 according to the number of samples to be tested. For protein quantification, 0, 1, 2, 4, 8, 12, 16, and 20 μL of the standard solution were added to the standard wells of a 96-well plate, and standard diluent was added to bring the final volume in each well to 20 μL. An appropriate volume of each sample was added to the sample wells, and if the sample volume was less than 20 μL, standard diluent was added to adjust the final volume to 20 μL. Subsequently, 200 μL of BCA working solution was added to each well, and the plate was incubated at 37 °C for 20−30 min. Absorbance was measured at 540 and 595 nm using a mircoplate reader. The protein concentration of each sample was calculated based on the standard curve and the sample volume used.

### 4.4. Western Blot (WB)

Purified salivary EV samples were lysed by adding SDS-PAGE sample loading buffer (P0015L, Beyotime Biotechnology) and heated at 100 °C for 10 min to ensure complete protein denaturation. After cooling to room temperature, samples were loaded onto gels at either equal volume (30 μL per lane) or equal protein amount (2 μg per lane), depending on the experimental design. Proteins were separated in a 10% sodium dodecyl sulfate-polyacrylamide gel (SDS-PAGE) and transferred onto a polyvinlindene fluoride (PVDF) membrane (10600023, GE Healthcare Life Science). The membranes were blocked with 5% nonfat milk at room temperature for 2 h and then incubated overnight at 4 °C with primary antibodies against Alix (1:1000, SC-53540, Santa Cruz Biotechnology), CD63 (1:1000, ab134045, Abcam), Flotillin 1 (1:1000, 610820, BD Biosciences), CD81 (1:1000, SC-166029, Santa Cruz Biotechnology), albumin (1:1000, SC-271604, Santa Cruz Biotechnology) and amylase (1:1000, SC-166349, Santa Cruz Biotechnology). After washing, the membrane were incubated with horseradish peroxidase (HRP)-conjugated anti-mouse or anti-rabbit IgG secondary antibodies (1:3000, 7076S/7074S, Cell Signaling Technology) for 1 h at room temperature. Following additional washing steps, protein bands were visualized using enhanced chemiluminescence (ECL) substrate (Pei Qing Science & Technology). Chemiluminescent signals were detected using a JS-M8 imaging system (JS-M8, Pei Qing Science & Technology, Shanghai, China).

### 4.5. Nanoparticle Tracking Analysis (NTA)

NTA was performed according to the manufacturer's instructions using a NanoSight NS300 system (Malvern Panalytical, Malvern, UK) equipped with with a high-sensitivity scientific sCMOS camera. For analysis of salivary EVs, samples were diluted in particle-free PBS to achieve particle concentrations within the optimal detection range of the instrument ($10^7$−$10^9$ particles/mL). A syringe pump was used to ensure constant-flow injection during measurement. For each sample, three 30 s videos were recorded and analyzed using NTA software (version 2.3) to determine the particle size distribution, particle concentration, and mean and mode particle sizes. The laser chamber was thoroughly cleaned between measurements using filtered deionized water to prevent cross-contamination.

### 4.6. Transmission Electron Microscope (TEM)

For TEM analysis, 20 μL of salivary EV samples were deposited onto 200-mesh Formvar/carbon-coated copper grids (BZ11022a, Beijing Zhongjingkeyi Technology Co., Ltd.) and incubated at room temperature for 30 min to allow adsoprtion. Excess liquid was removed with filter paper, and the grids were air-dry for 1 h. The samples were then negatively stained with filtered 3% (w/v) aqueous uranyl acetate (GZ02625, Beijing Zhongjingkeyi Technology Co., Ltd.) for 30 s. The staining solution was freshly prepared and filtered through a 0.22 μm membrane before use. After staining, excess dye was carefully blotted with filter paper, and the grids were dried under vacuum. The samples were subsequantly characterized using TEM (FEI Tecnai) operated at an accelerating voltage of 100 kV.

### 4.7. TMT-Based Proteomics for Protein Identification and Quantification

(a) Protein extraction: Salivary EV samples were lysed in lysis buffer containing 8 M urea and 1% protease inhibitor, followed by sonication . Insoluble debris was removed by centrifugation at 12,000 × *g* for 10 min at 4 °C. The supernatant was collected, and protein concentration was determined using a BCA kit. (b) Protein digestion: Protein samples were reduced with 5 mM dithiothreitol (DTT) at 56 °C for 30 min and alkylated with 11 mM iodoacetamide (IAA) at room temperature for 15 min in the dark. The samples were transferred to ultrafiltration tubes and centrifuged at 12,000 × *g* for 20 min. Trypsin was added at a 1:50 (w/w) enzyme-to-protein ratio, and digestion was performed overnight at 37 °C. (c) TMT labeling: Following digestion, peptides were desalted using a Strata X C18 SPE column (Phenomenex) and vacuum-dried. Each TMT reagent vial was dissolved in 41 μL of LC-MS-grade ACN, and the peptides were incuated with the TMT reagents for 1 h at room temperature. The labeled samples were then pooled and and dried by vacuum centrifugation. (d) High-pH reverse-phase fractionation: Peptides were fractionated by high-pH-reverse-phase high-performace liquid chromatography (HPLC) using a gradient of 8%−32% ACN over 1h, yielding 60 fractions. These fractions were subsequently combined into 14 components and dried by vacuum centrifugation. . (e) LC-MS/MS analysis: Peptides were reconstituted in buffer A (0.1% formic acid (FA) and 2% ACN) and separated using an EASY-nLC 1000 system. The separated peptides were ionized using a nanoelectrospray ionization (NSI) source and analyzed on a for ionizion and then analyzed on Q_Exactive Plus mass spectrometer (Thermo Fisher Scientific). The ion source voltage was set at 2.2 kV. MS1 scans were acquired over a mass range of 400−1500 $m/z$ at resolution of 70,000, and MS2 scans were acquired at a resolution of 17,500. (f) Database search and protein quantification: MS/MS


https://doi.org/10.1021/acsnano.5c20621
ACS Nano XXXX, XXX, XXX−XXX

spectra were processed using MaxQuant (v1.5.2.8). The search was performed against parameter the Homo sapiens database (Homo_sapiens_9606_SP_20191115, 20,380 entries). Trypsin/P was specified as the digestion enzyme, allowing 2 missed cleavages. The minimum peptide length was set to 7 amino acids, up to 5 variablemodifications were permitted. The precursor ion mass tolerance was set to 20ppm for the first search and 5 ppm for the main search, while the fragment ion tolerance was set to 0.02 Da. TMT-6 plex labeling was used for quantification. The false discovery rate (FDR) for both protein and peptide-spectru match (PSM) identification was set to 1%.

### 4.8. Data Acquisition and Analysis of EC Patientsc

Clinical data and mRNA expression profiles of EC patients were obtained from The Cancer Genome Atals (TCGA) database, including 165 tumor samples and 13 normal tissue samples. The TCGA-EC cohort is publicly available at the GDC Data Portal (https://portal.gdc.cancer.gov/). RNA-seq data originally provided in fragments per kilobase of transcript per million mapped reads (FPKM) format were converted to transcripts per million (TPM) format and subsequently log2-transformed for downstream analysis. Differential expression analysis was performed using the DESeq2 R package. A diagnostic gene model for EC and early-stage (defined as T1, N0, and stage I) was initially developed using the TCGA cohort. To further optimize and validate the model, an independent healthy control cohort comprising 649 individuals from the Genotype-Tissue Expression (GTEx) dataset (https://xenabrowser.net/datapages/) was included. In addtion, a prospectively collected cohort consisting of 24 healthy volunteers and 24 newly diagnosed EC patients was used to further validate the diagnostic performace of the selected gene markers. Western blot analysis was performed using a ProteinSimple Wes capillary-based automatic Western blot system (ProteinSimple, USA).

### 4.9. Statistical Analysis

All data are presented as the mean ± standard error of the mean (SEM). Statistical comparisions between two groups were performed using a two-tailed Student's *t*-test (paired or unpaired, as appropriate). Linear regression analysis was conducted to assess relationships between variables. Statistical significance was defined as $p < 0.05$. All analyses were performed using R software (https://www.r-project.org/,version 4.0.5), with relevant packages including limma, ggplot2, clusterProfile, DESeq2, pROC, and VennDiagram. Logistic regression (LR), receiver operating characteristic (ROC) analysis, and area under the curve (AUC) calculations were performed to evaluate diagnostic performance.

## ■ ASSOCIATED CONTENT

### Supporting Information

The Supporting Information is available free of charge at https://pubs.acs.org/doi/10.1021/acsnano.5c20621.

Detailed experimental procedures, supplementary methods, additional figures (Figures S1−S9), and supplementary tables (Tables S1−S11) (PDF)

## ■ AUTHOR INFORMATION


### Corresponding Authors

**Tony Y. Hu** − *School of Biomedical Engineering, Tsinghua Medicine, Tsinghua University, Beijing 100084, China;* Present Address: Center for Cellular and Molecular Diagnostics and Department of Biochemistry and Molecular Biology, Tulane University School of Medicine, New Orleans, Louisiana 70112, United States; orcid.org/0000-0002-5166-4937; Email: tony_hu@mail.tsinghua.edu.cn

**Luke P. Lee** − *Department of Medicine, Brigham and Women's Hospital, Harvard Medical School, Boston, Massachusetts 02115, United States; Department of Bioengineering, Department of Electrical Engineering and Computer Science, University of California, Berkeley, Berkeley, California 94720, United States; Institute of Quantum Biophysics, Department of Biophysics, Sungkyunkwan University, Suwon 16419, Korea;* orcid.org/0000-0002-1436-4054; Email: lplee@bwh.harvard.edu

**Fei Liu** − *Department of Medicine, Brigham and Women's Hospital, Harvard Medical School, Boston, Massachusetts 02115, United States;* orcid.org/0000-0001-5259-5753; Email: fliu@bwh.harvard.edu

### Authors

**Liu Huang** − *Department of Oncology, Tongji Hospital, Tongji Medical College, Huazhong University of Science and Technology, Wuhan, Hubei 430030, China*

**Meng Li** − *Eye Hospital, School of Ophthalmology & Optometry, School of Biomedical Engineering, Wenzhou Medical University, Wenzhou, Zhejiang 325035, China*

**Wenpeng Liu** − *School of Biomedical Engineering, Tsinghua Medicine, Tsinghua University, Beijing 100084, China;* orcid.org/0000-0002-2932-1321

**Doudou Lou** − *Eye Hospital, School of Ophthalmology & Optometry, School of Biomedical Engineering, Wenzhou Medical University, Wenzhou, Zhejiang 325035, China*

**Qingfu Zhu** − *Eye Hospital, School of Ophthalmology & Optometry, School of Biomedical Engineering, Wenzhou Medical University, Wenzhou, Zhejiang 325035, China;* orcid.org/0000-0003-1065-0739

Complete contact information is available at: https://pubs.acs.org/10.1021/acsnano.5c20621


### Author Contributions

[¶]L.H. and M.L. contributed equally to this work. T.H., L.P.L., and F.L. conceived the project and designed the experiments. L.H. and M.L. organized and collected clinical samples. M.L. purified and characterized salivary EVs. F.L., M.L., D.L., W.L., and Q.Z. contributed to data analysis and interpretation. M.L., L.H., D.L., W.L., and Q.Z. wrote the original manuscript. F.L., L.P.L., and T.H. edited the manuscript. All experiments were conducted under the supervision of T.H., L.P.L., and F.L. All authors have read and approved the final manuscript.

### Notes

The authors declare the following competing financial interest(s): Fei Liu is a co-founder of Huixin Lifetech.

## ■ ACKNOWLEDGMENTS

The work was supported by the research funds provided by the Zhejiang Provincial and Ministry of Health Research Fund for Medical Sciences (WKJ-ZJ-1910), the National Natural Science Foundation of China (81602104, 31901043), and the Wenzhou Medical University (89218012).

## ■ ABBREVIATIONS

BP, biological processes; CC, cellular component; EXODUS, exosome detection via the ultrafast-isolation system; EC, Esophageal cancer; GO, Gene ontology; KEGG, the Kyoto Encyclopedia of Genes and Genomes; MF, molecular functions; NTA, nanoparticle tracking analysis; PBS, phosphate buffer solution; PCA, principal component analysis; PEG, polyethylene glycol precipitation; TEM, transmission

electron microscopy; TMT, tandem mass tag; UC, ultracentrifugation; WB, Western blotting

## REFERENCES


(1) (a) Bray, F.; Ferlay, J.; Soerjomataram, I.; Siegel, R. L.; Torre, L. A.; Jemal, A. Global cancer statistics 2018: GLOBOCAN estimates of incidence and mortality worldwide for 36 cancers in 185 countries. *Ca-Cancer J. Clin.* **2018**, *68* (6), 394−424. (b) Zhou, X.; Gao, F.; Gao, W.; Wang, Q.; Li, X.; Li, X.; Li, W.; Liu, J.; Zhou, H.; Luo, A.; et al. Bismuth Sulfide Nanoflowers Facilitated miR339 Delivery to Overcome Stemness and Radioresistance through Ubiquitin-Specific Peptidase 8 in Esophageal Cancer. *ACS Nano* **2024**, *18* (29), 19232−19246. (c) Zhou, L.-L.; Guan, Q.; Zhou, W.; Kan, J.-L.; Teng, K.; Hu, M.; Dong, Y.-B. A Multifunctional Covalent Organic Framework Nanozyme for Promoting Ferroptotic Radiotherapy against Esophageal Cancer. *ACS Nano* **2023**, *17* (20), 20445−20461. (d) Shi, G.; Cui, Y.; Zhao, J.; Liu, J.; Wang, Y.; Yang, Y.; Han, J.; Cheng, X.; Chen, L.; Yuan, Y.; et al. Identifying TOPK and Hypoxia Hallmarks in Esophageal Tumors for Photodynamic/Chemo/Immunotherapy and Liver Metastasis Inhibition with Nanocarriers. *ACS Nano* **2023**, *17* (7), 6193−6207.

(2) Abnet, C. C.; Arnold, M.; Wei, W. Q. Epidemiology of Esophageal Squamous Cell Carcinoma. *Gastroenterology* **2018**, *154* (2), 360−373.

(3) He, Y.; Quaresma, M.; dos-Santos-Silva, I. Stage-Specific Survival From Esophageal Cancer in China and Implications for Control Strategies: A Systematic Review and Meta-Analyses. *Gastro Hep Advances* **2023**, *2* (3), 426−437.

(4) (a) Tenchov, R.; Sasso, J. M.; Wang, X.; Liaw, W. S.; Chen, C. A.; Zhou, Q. A. Exosomes horizontal line Nature's Lipid Nanoparticles, a Rising Star in Drug Delivery and Diagnostics. *ACS Nano* **2022**, *16* (11), 17802−17846. (b) Sharma, S.; Rasool, H. I.; Palanisamy, V.; Mathisen, C.; Schmidt, M.; Wong, D. T.; Gimzewski, J. K. Structural-mechanical characterization of nanoparticle exosomes in human saliva, using correlative AFM, FESEM, and force spectroscopy. *ACS Nano* **2010**, *4* (4), 1921−1926. (c) Li, Z.; Chen, F.; Zhu, N.; Zhang, L.; Xie, Z. Tip-Enhanced Sub-Femtomolar Steroid Immunosensing via Micropyramidal Flexible Conducting Polymer Electrodes for At-Home Monitoring of Salivary Sex Hormones. *ACS Nano* **2023**, *17* (21), 21935−21946.

(5) (a) Qi, H.; Liu, C.; Long, L.; Ren, Y.; Zhang, S.; Chang, X.; Qian, X.; Jia, H.; Zhao, J.; Sun, J.; et al. Blood Exosomes Endowed with Magnetic and Targeting Properties for Cancer Therapy. *ACS Nano* **2016**, *10* (3), 3323−3333. (b) Ibsen, S. D.; Wright, J.; Lewis, J. M.; Kim, S.; Ko, S.-Y.; Ong, J.; Manouchehri, S.; Vyas, A.; Akers, J.; Chen, C. C.; et al. Rapid Isolation and Detection of Exosomes and Associated Biomarkers from Plasma. *ACS Nano* **2017**, *11* (7), 6641−6651.

(6) Han, Y.; Jia, L.; Zheng, Y.; Li, W. Salivary Exosomes: Emerging Roles in Systemic Disease. *Int. J. Biol. Sci.* **2018**, *14* (6), 633−643.

(7) Li, M.; Lou, D.; Chen, J.; Shi, K.; Wang, Y.; Zhu, Q.; Liu, F.; Zhang, Y. Deep dive on the proteome of salivary extracellular vesicles: comparison between ultracentrifugation and polymer-based precipitation isolation. *Anal. Bioanal. Chem.* **2021**, *413* (2), 365−375.

(8) Nagler, R.; Bahar, G.; Shpitzer, T.; Feinmesser, R. Concomitant analysis of salivary tumor markers–a new diagnostic tool for oral cancer. *Clin. Cancer Res.* **2006**, *12* (13), 3979−3984.

(9) Zhou, P.; Lu, F.; Wang, J.; Wang, K.; Liu, B.; Li, N.; Tang, B. A portable point-of-care testing system to diagnose lung cancer through the detection of exosomal miRNA in urine and saliva. *Chem. Commun.* **2020**, *56* (63), 8968−8971.

(10) Lau, C.; Kim, Y.; Chia, D.; Spielmann, N.; Eibl, G.; Elashoff, D.; Wei, F.; Lin, Y. L.; Moro, A.; Grogan, T.; et al. Role of pancreatic cancer-derived exosomes in salivary biomarker development. *J. Biol. Chem.* **2013**, *288* (37), 26888−26897.

(11) Wood, N.; Streckfus, C. F. The expression of lung resistance protein in saliva: a novel prognostic indicator protein for carcinoma of the breast. *Cancer Invest.* **2015**, *33* (10), 510−515.

(12) Lin, Y.; Dong, H.; Deng, W.; Lin, W.; Li, K.; Xiong, X.; Guo, Y.; Zhou, F.; Ma, C.; Chen, Y.; et al. Evaluation of Salivary Exosomal Chimeric GOLM1-NAA35 RNA as a Potential Biomarker in Esophageal Carcinoma. *Clin. Cancer Res.* **2019**, *25* (10), 3035−3045.

(13) Xie, Z.; Chen, G.; Zhang, X.; Li, D.; Huang, J.; Yang, C.; Zhang, P.; Qin, Y.; Duan, Y.; Gong, B.; et al. Salivary microRNAs as promising biomarkers for detection of esophageal cancer. *PLoS One* **2013**, *8* (4), No. e57502.

(14) (a) Dey, K. K.; Wang, H.; Niu, M.; Bai, B.; Wang, X.; Li, Y.; Cho, J. H.; Tan, H.; Mishra, A.; High, A. A.; et al. Deep undepleted human serum proteome profiling toward biomarker discovery for Alzheimer's disease. *Clin. Proteomics* **2019**, *16*, 16. (b) Macron, C.; Lane, L.; Nunez Galindo, A.; Dayon, L. Deep Dive on the Proteome of Human Cerebrospinal Fluid: A Valuable Data Resource for Biomarker Discovery and Missing Protein Identification. *J. Proteome Res.* **2018**, *17* (12), 4113−4126.

(15) Hu, S.; Chen, B.; Zhou, J.; Liu, F.; Mao, T.; Pathak, J. L.; Watanabe, N.; Li, J. Dental pulp stem cell-derived exosomes revitalize salivary gland epithelial cell function in NOD mice via the GPER-mediated cAMP/PKA/CREB signaling pathway. *J. Transl. Med.* **2023**, *21* (1), 361.

(16) Yakubovich, E. I.; Polischouk, A. G.; Evtushenko, V. I. Principles and Problems of Exosome Isolation from Biological Fluids. *Biochem. (Moscow), Suppl. Ser.* **2022**, *16* (2), 115−126.

(17) Piffoux, M.; Silva, A. K. A.; Wilhelm, C.; Gazeau, F.; Tareste, D. Modification of Extracellular Vesicles by Fusion with Liposomes for the Design of Personalized Biogenic Drug Delivery Systems. *ACS Nano* **2018**, *12* (7), 6830−6842.

(18) (a) Wang, Z.; Li, F.; Rufo, J.; Chen, C.; Yang, S.; Li, L.; Zhang, J.; Cheng, J.; Kim, Y.; Wu, M.; et al. Acoustofluidic Salivary Exosome Isolation: A Liquid Biopsy Compatible Approach for Human Papillomavirus-Associated Oropharyngeal Cancer Detection. *J. Mol. Diagn.* **2020**, *22* (1), 50−59. (b) Yuyang Gu, C. C.; Mao, Z.; Bachman, H.; Becker, R.; et al. Acoustofluidic centrifuge for nanoparticle enrichment and separation. *Sci. Adv.* **2021**, *7*, No. eabc0467. (c) Wang, Z.; Rich, J.; Hao, N.; Gu, Y.; Chen, C.; Yang, S.; Zhang, P.; Huang, T. J. Acoustofluidics for simultaneous nanoparticle-based drug loading and exosome encapsulation. *Microsyst. Nanoeng.* **2022**, *8*, 45. (d) Zhang, P.; Zhou, X.; He, M.; Shang, Y.; Tetlow, A. L.; Godwin, A. K.; Zeng, Y. Ultrasensitive detection of circulating exosomes with a 3D-nanopatterned microfluidic chip. *Nat. Biomed. Eng.* **2019**, *3* (6), 438−451. (e) Naquin, Ty D.; Canning, A. J.; Gu, Y.; Chen, J.; Naquin, C. M.; Xia, J.; Lu, B.; Yang, S.; Koroza, A.; Lin, K.; Wang, H.-N.; Jeck, W. R.; Lee, L. P.; Vo-Dinh, T.; Huang, Y. J. Acoustic separation and concentration of exosomes for nucleotide detection: ASCENDx. *Sci. Adv.* **2024**, *10*, 8597. (f) Zhao, Z.; Yang, Y.; Zeng, Y.; He, M. A Microfluidic ExoSearch Chip for Multiplexed Exosome Detection Towards Blood-based Ovarian Cancer Diagnosis. *Lab Chip* **2016**, *16* (3), 489−496.

(19) Chen, Y.; Zhu, Q.; Cheng, L.; Wang, Y.; Li, M.; Yang, Q.; Hu, L.; Lou, D.; Li, J.; Dong, X.; et al. Exosome detection via the ultrafast-isolation system: EXODUS. *Nat. Methods* **2021**, *18* (2), 212−218.

(20) (a) Hu, L.; Zhang, T.; Ma, H.; Pan, Y.; Wang, S.; Liu, X.; Dai, X.; Zheng, Y.; Lee, L. P.; Liu, F. Discovering the Secret of Diseases by Incorporated Tear Exosomes Analysis via Rapid-Isolation System: iTEARS. *ACS Nano* **2022**, *16* (8), 11720−11732. (b) Zhu, Q.; Luo, J.; Li, H. P.; Ye, W.; Pan, R.; Shi, K. Q.; Yang, R.; Xu, H.; Li, H.; Lee, L. P.; et al. Robust Acute Pancreatitis Identification and Diagnosis: RAPIDx. *ACS Nano* **2023**, *17* (9), 8564−8574.

(21) Tian, Y.; Ma, L.; Gong, M.; Su, G.; Zhu, S.; Zhang, W.; Wang, S.; Li, Z.; Chen, C.; Li, L.; et al. Protein Profiling and Sizing of Extracellular Vesicles from Colorectal Cancer Patients via Flow Cytometry. *ACS Nano* **2018**, *12* (1), 671−680.

(22) Huo, Y.; Cao, K.; Kou, B.; Chai, M.; Dou, S.; Chen, D.; Shi, Y.; Liu, X. TP53BP2: Roles in suppressing tumorigenesis and therapeutic opportunities. *Genes Dis.* **2023**, *10* (5), 1982−1993.

(23) Pan, X.; Wang, J.; Guo, L.; Na, F.; Du, J.; Chen, X.; Zhong, A.; Zhao, L.; Zhang, L.; Zhang, M.; et al. Identifying a confused cell




https://doi.org/10.1021/acsnano.5c20621
*ACS Nano* XXXX, XXX, XXX−XXX

identity for esophageal squamous cell carcinoma. *Signal Transduct. Targeted Ther.* **2022**, *7* (1), 122.
(24) Fucikova, J.; Spisek, R.; Kroemer, G.; Galluzzi, L. Calreticulin and cancer. *Cell Res.* **2021**, *31* (1), 5−16.
(25) Zhang, C.; Chang, X.; Chen, D.; Yang, F.; Li, Z.; Li, D.; Yu, N.; Yan, L.; Liu, H.; Xu, Z. Downregulation of HDGF inhibits the tumorigenesis of bladder cancer cells by inactivating the PI3K-AKT signaling pathway. *Cancer Manage. Res.* **2019**, *11*, 7909−7923.
(26) Peng, Y.; Tang, Q.; Xiao, F.; Fu, N. Regulation of Lipid Metabolism by Lamin in Mutation-Related Diseases. *Front. Pharmacol.* **2022**, *13*, 820857.
(27) Zhu, Q.; Xu, H.; Huang, L.; Luo, J.; Li, H.; Yang, R.; Liu, X.; Liu, F. Identification and detection of plasma extracellular vesicles-derived biomarkers for esophageal squamous cell carcinoma diagnosis. *Biosens. Bioelectron.* **2023**, *225*, 115088.
(28) Zhu, Q.; Huang, L.; Yang, Q.; Ao, Z.; Yang, R.; Krzesniak, J.; Lou, D.; Hu, L.; Dai, X.; Guo, F.; et al. Metabolomic analysis of exosomal-markers in esophageal squamous cell carcinoma. *Nanoscale* **2021**, *13* (39), 16457−16464.
(29) Jing, Z.; Guo, Z.; Zhang, C. Plasma-derived Exosomal miR-25−3p and miR-23b-3p as Predictors of Response to Chemoradiotherapy in Esophageal Squamous Cell Carcinoma. *Technol. Cancer Res. Treat.* **2024**, *23*, 15330338241289520.
(30) Wang, Y.; Li, X.; Wei, X.; Li, L.; Bai, H.; Yan, X.; Zhang, H.; Zhao, L.; Zhou, W.; Zhao, L. Identification of combinatorial miRNA panels derived from extracellular vesicles as biomarkers for esophageal squamous cell carcinoma. *MedComm* **2023**, *4* (5), No. e377.
(31) Xing, S.; Zheng, X.; Wei, L.-Q.; Song, S.-J.; Liu, D.; Xue, N.; Liu, X.-M.; Wu, M.-T.; Zhong, Q.; Huang, C.-M.; et al. Development and Validation of a Serum Biomarker Panel for the Detection of Esophageal Squamous Cell Carcinoma through RNA Transcriptome Sequencing. *J. Cancer* **2017**, *8* (12), 2346−2355.
(32) Tong, Y.-S.; Wang, X.-W.; Zhou, X.-L.; Liu, Z.-H.; Yang, T.-X.; Shi, W.-H.; Xie, H.-W.; Lv, J.; Wu, Q.-Q.; Cao, X.-F. Identification of the long non-coding RNA POU3F3 in plasma as a novel biomarker for diagnosis of esophageal squamous cell carcinoma. *Mol. Cancer* **2015**, *14*, 3.
(33) Miyoshi, J.; Zhu, Z.; Luo, A.; Toden, S.; Zhou, X.; Izumi, D.; Kanda, M.; Takayama, T.; Parker, I. M.; Wang, M.; et al. A microRNA-based liquid biopsy signature for the early detection of esophageal squamous cell carcinoma: a retrospective, prospective and multicenter study. *Mol. Cancer* **2022**, *21* (1), 44.
(34) (a) Li, K.; Lin, Y.; Luo, Y.; Xiong, X.; Wang, L.; Durante, K.; Li, J.; Zhou, F.; Guo, Y.; Chen, S.; et al. A signature of saliva-derived exosomal small RNAs as predicting biomarker for esophageal carcinoma: a multicenter prospective study. *Mol. Cancer* **2022**, *21* (1), 21. (b) Rao, D.; Lu, H.; Wang, X.; Lai, Z.; Zhang, J.; Tang, Z. Tissue-derived exosome proteomics identifies promising diagnostic biomarkers for esophageal cancer. *eLife* **2023**, *12*, No. e86209.




https://doi.org/10.1021/acsnano.5c20621
*ACS Nano* XXXX, XXX, XXX−XXX